

## Graphical Abstract

**Solvent effects on the prediction of redox potentials: application to nitroxides**

Pierre Beaujean

## Highlights

**Solvent effects on the prediction of redox potentials: application to nitroxides**

Pierre Beaujean

- Research highlight 1
- Research highlight 2

# Solvent effects on the prediction of redox potentials: application to nitroxides

Pierre Beaujean<sup>a,\*</sup>

<sup>a</sup>*Theoretical Chemistry Laboratory, Unit of Theoretical and Structural Physical Chemistry,  
Namur Institute of Structured Matter, University of Namur, Rue de Bruxelles,  
61, Namur, B-5000, Belgium*

---

## Abstract

This is an abstract

*Keywords:*

---

## 1. Introduction

This is an introduction. It will contain:

- Batteries
- Nitroxides [1], Fig. 1
- Prediction of redox potential, and **the needs for a correct description of solvent-solute interactions**
- So: SMD, then Debye-Huckel, then CIP (or Matsui)

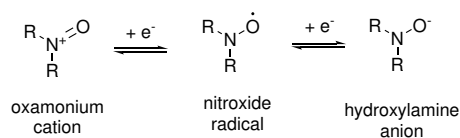


Figure 1: Oxidized (left) and reduced (right) form of the the nitroxide radical (center).

---

\*Corresponding author

Email address: pierre.beaujean@unamur.be (Pierre Beaujean)

## 2. Theory

### 2.1. Redox potential of an ion in solution

According to Ref. [2], the absolute reduction potential  $E_{abs}^0$  (in V) of the half-reaction of reduction of  $X^z$ ,  $X^z + n_e e^- \rightarrow X^{z-n_e}$ , reads:

$$E_{abs}^0(X^z|X^{z-n_e}) = -\frac{\Delta G_r^*}{n_e F}, \text{ with } \Delta G_r^* = G^*(X^{z-n_e}) - G^*(X^z), \quad (1)$$

where  $\Delta G_r^*$  is the free Gibbs energy of the reduction reaction in solution,  $F$  is the Faraday constant and  $n_e$  the number of electrons involved in the reduction process. Last but not least,  $G^*(X^z)$  is the Gibbs free energy of  $X^z$  in solution. In the rest of this article, it is considered that  $G^*(e^-) = 0$ .

From a phenomenological point of view, such energy is the sum of the one of the system in vacuum, plus the change in (free) energy resulting from its transfer to an electrolytic solution, *i.e.*,  $G^*(X^z) = G^0(X^z) + \Delta G_S^*(X^z)$ . The latter may be further decomposed using the thermodynamic cycle presented in Figure 2. There are four steps:  $\Delta G_d + \Delta G_s$  (discharge of a sphere in gas phase followed by charge in a dielectric) is a purely electrostatic processes, while  $\Delta G_s$  is due, in most part, to non-electrostatic contributions (cavitation, vdW, etc). Finally,  $\Delta G_{DH}^*$  adds the effect of surrounding ions, and is therefore important to treat electrolytes [3].

On the one hand, at the quantum chemistry (QC) level, the solvation energy is generally treated implicitly, thanks to a self-consistent reaction field approach (SCRF) [4]:

$$\begin{aligned} G_{SCRF}^*(X) &= \left\langle \Psi \left| \hat{H} + \frac{1}{2} \hat{R} \right| \Psi \right\rangle + G_{th}[\Psi] + G_{nonelst}(X) \\ &= E[\Psi] + G_{th}[\Psi] + \underbrace{G_{elst}[\Psi] + G_{nonelst}(X)}_{\Delta G_{S,SCRF}^*(X)}, \end{aligned} \quad (2)$$

where  $\Psi$  is the wavefunction of  $X$  (minimized under the application of  $\hat{R}$ , so not equal to the gas phase wavefunction),  $\hat{H}$  is the electronic Hamiltonian,  $\hat{R}$  is the reaction field operator (generally recognized to give rise to the electrostatic contribution to the solvation energy,  $G_{elst}$ ),  $G_{th}$  are the thermal contributions

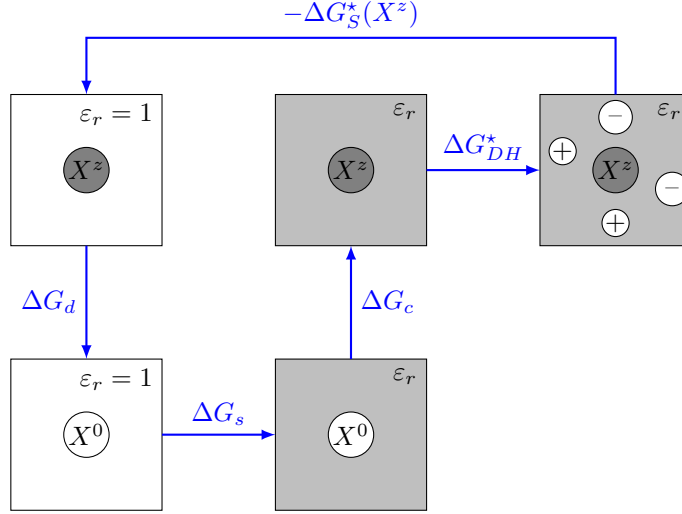


Figure 2: Thermodynamic cycle to compute the energy of solvation of an ion,  $X^z$ , in a electrolyte (solvent characterized by a  $\varepsilon = \varepsilon_0 \varepsilon_r$  dielectric constant and by a “cloud” of other ions).  $\Delta G_d$  is the discharge of  $X^z$  in gas phase,  $\Delta G_s$  is the solvation of  $X$ ,  $\Delta G_c$  is the charging of  $X$  in  $\varepsilon$ , and  $\Delta G_{DH}^*$  is the addition of the other ions.

to the Gibbs free energy derived from thermostatic analysis, and  $G_{nonelst}$  is the non-electrostatic contributions (cavitation, dispersion, etc) to the solvation energy. Therefore, using the notation of Figure 2 (and assuming no change in the geometry of  $X^z$ ),  $\Delta G_{S,SCRF}^*(X^z) = \Delta G_d + \Delta G_s + \Delta G_c$ .

On the other hand, the Debye-Huckel (DH) theory provide another estimate of  $\Delta G_S^*$  [5]. Indeed, assuming that a ion  $X^z$ , bearing a charge  $q = z e_0$  ( $e_0$  is the elementary charge), can be approximated by a sphere of radius  $a$  and that the ions in the solution are distributed in the solution according to Maxwell-Boltzmann statistics, one obtains the corresponding solvation energy as [6, 7, 3]:

$$\Delta G_{S,DH}^*(X^z) = \Delta G_{born}^*(X^z) + \Delta G_{DH}^*(X^z) \quad (3)$$

where:

$$\Delta G_{born}^*(X^z) = \frac{q^2}{8\pi\varepsilon_0 a} \left[ \frac{1}{\varepsilon_r} - 1 \right], \quad (4)$$

and,

$$\Delta G_{DH}^*(X^z) = -\frac{q^2}{4\pi\epsilon_0\epsilon_r} \frac{\kappa}{(\kappa a)^3} \left[ \ln(1 + \kappa a) - \kappa a + \frac{1}{2}(\kappa a)^2 \right], \quad (5)$$

in which  $\kappa$  is the inverse of the Debye screening length, defined from:

$$\kappa^2 = \sum_i \frac{n_i q_i^2}{\epsilon_0 \epsilon_r k_B T}, \quad (6)$$

where  $n_i$  is the number density ( $n_i = N_i/V = c_i \mathcal{N}_a$  where  $\mathcal{N}_a$  is the Avogadro number and  $c_i$  is the concentration in ion  $i$ ) of ion of type  $i$ ,  $k_B$  is the Boltzmann constant, and  $T$  is the temperature.  $\kappa$  is proportional to the ionic strength of the solution,  $I = \frac{1}{2} \sum_i c_i z_i^2$ .

In the limit of  $\kappa \rightarrow 0$ ,  $\Delta G_{DH}^* = 0$  and thus  $\Delta G_S^* \approx \Delta G_{born}^* = \Delta G_d + \Delta G_c$ . Therefore, by combining Eqs. (2) and (3), one defines:

$$G^*(X^z) = G_{SCRF}^*(X^z) + \Delta G_{DH}^*(X^z), \quad (7)$$

to be used in Eq. (1). It should provide similar results to the approach developed by Cossi *et al.* in Ref. 8.

## 2.2. Model for the ion-pair formation

To further model the impact of the electrolyte on the redox potential, the formation of ion pairs is also considered (Fig. 3). Here, the electrolyte is composed of a pair AC, where  $A^-$  and  $C^+$  are a cation and an ion, respectively. Being favored by electrostatic interactions, the close-contact pairing of the oxidized ( $N^+$ ) and reduced ( $N^-$ ) state of nitroxide ( $N^\bullet$ ) with its corresponding counterion ( $A^-$  and  $C^+$ , respectively) is first considered. Then, further complexation with the AC pair in close contact is considered [9].

Assumptions:

- Redox process for ion pair is negligible (to be checked).
- $C_{N^+} = [N^+] + [NA] + [NAC^+]$ , etc.
- At equilibrium,  $C_{N^+} = C_{N^\bullet}$ , etc.



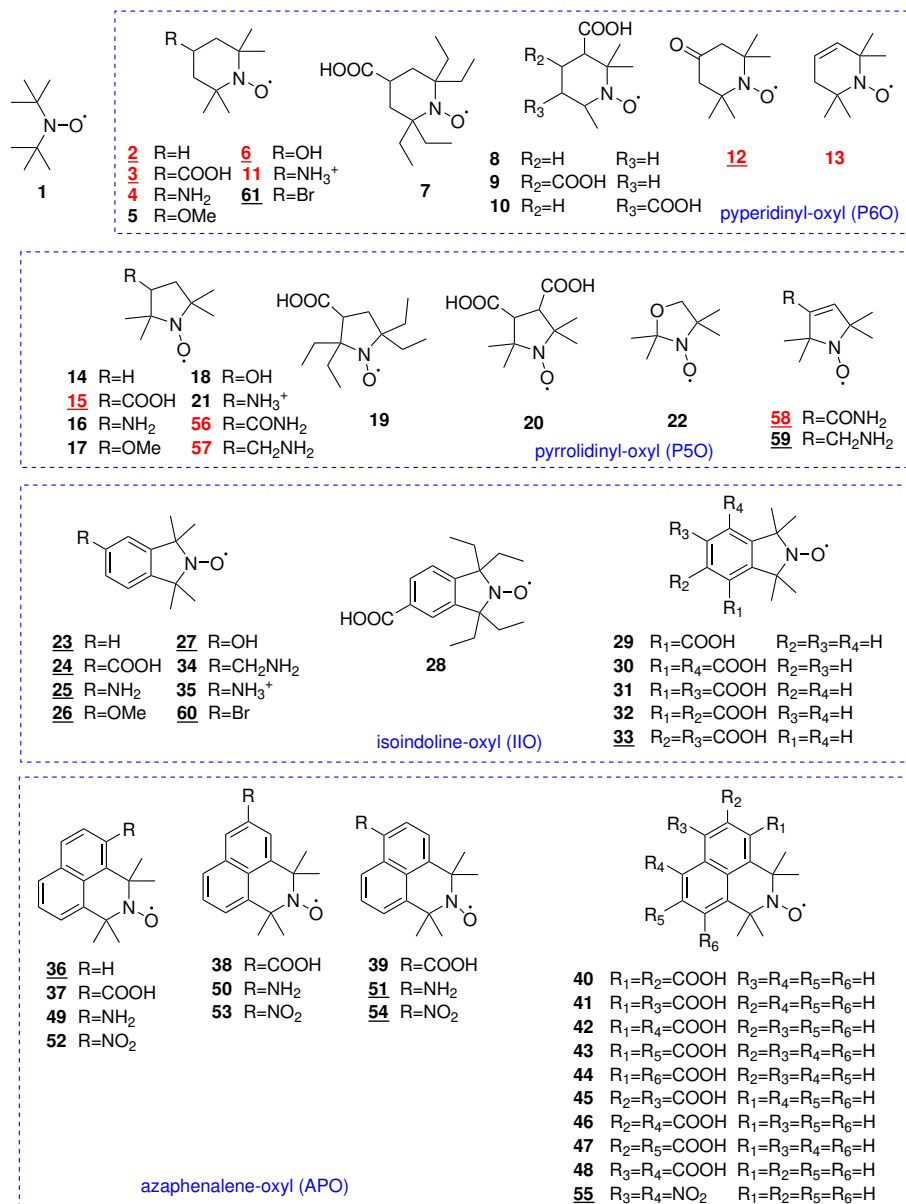


Figure 4: The different nitroxides considered in this work, sorted by families. Compounds **1-54** are from Ref. 10, while compounds **55-61** were considered for completeness. Experimental (reduction or oxidation) potentials are available in water if the number is written in red, while they are available in acetonitrile if the number is underlined.



considered to have a doublet ground state. Then, the compounds for which there are experimental redox potentials available in acetonitrile (see Figure 4), geometry optimization and vibrational frequency calculations were also performed in this solvent.

In this work, a value of  $\varepsilon_r = 80$  ( $\varepsilon_r = 35$ ) is used for water (acetonitrile). These relative permittivities are the one of pure solvent, and are known to be lower in corresponding electrolytes [13]. These variations can be, indeed, quite substantial (for example,  $\varepsilon \approx 70$  for a solution containing  $1 \text{ mol kg}^{-1}$  of NaCl in water [6, 13]), but they are also strongly dependent on the nature of the electrolyte.

#### 4. Results and discussion

- Structure-activity relationships, on simple results (Fig. 5), if possible (see Hodgson et al [10]). Also, comparing water and acetonitrile (Fig. 7).
- low-concentration limit: DH corrections
- High-concentration limit: CIP (also, structure-activity relationship for CIP!) and Matsui.
- Comparison to experiment

#### 5. Conclusion

Well.

#### References

- [1] B. P. Soule, F. Hyodo, K.-i. Matsumoto, N. L. Simone, J. A. Cook, M. C. Krishna, J. B. Mitchell, The chemistry and biology of nitroxide compounds, *Free Radical Biology and Medicine* 42 (2007) 1632–1650. doi:10.1016/j.freeradbiomed.2007.02.030.

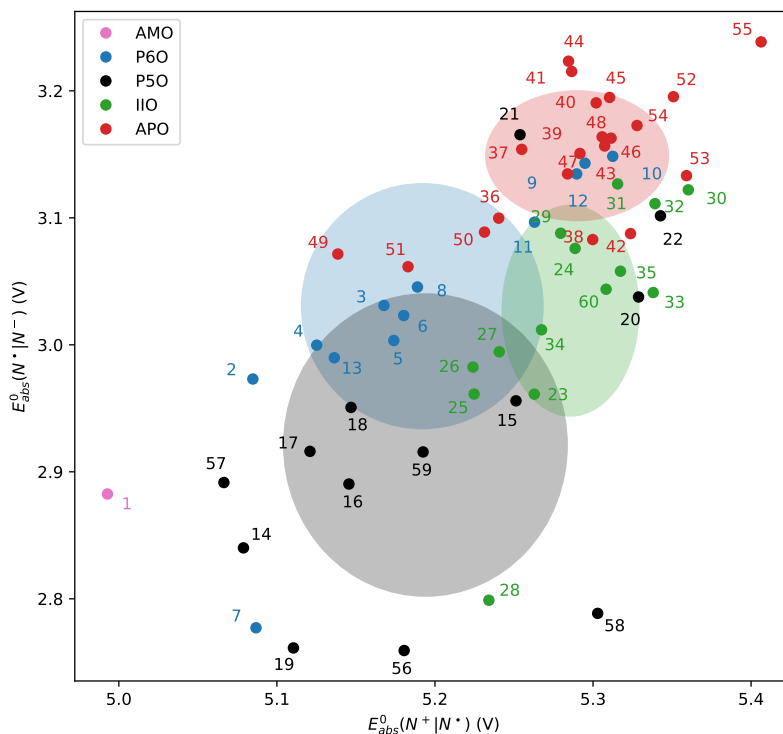


Figure 5: Relationship between absolute oxidation and reduction potentials of nitroxides, as computed at the  $\omega$ B97X-D/6-311+G(d) level in water (SMD), with  $[X] = 0 \text{ mol L}^{-1}$ . The color indicate the family (Fig. 4). For each of them, an ellipse is drawn, centered on the mean potential value among the family, and which width and height are given by the standard deviations.

- [2] A. V. Marenich, J. Ho, M. L. Coote, C. J. Cramer, D. G. Truhlar, Computational electrochemistry: Prediction of liquid-phase reduction potentials, *Physical Chemistry Chemical Physics* 16 (2014) 15068–15106. doi:10.1039/C4CP01572J.
- [3] G. M. Silva, B. Maribo-Mogensen, X. Liang, G. M. Kontogeorgis, Improving the Born equation: Origin of the Born radius and introducing dielectric saturation effects, *Fluid Phase Equilibria* 576 (2024) 113955. doi:10.1016/j.fluid.2023.113955.

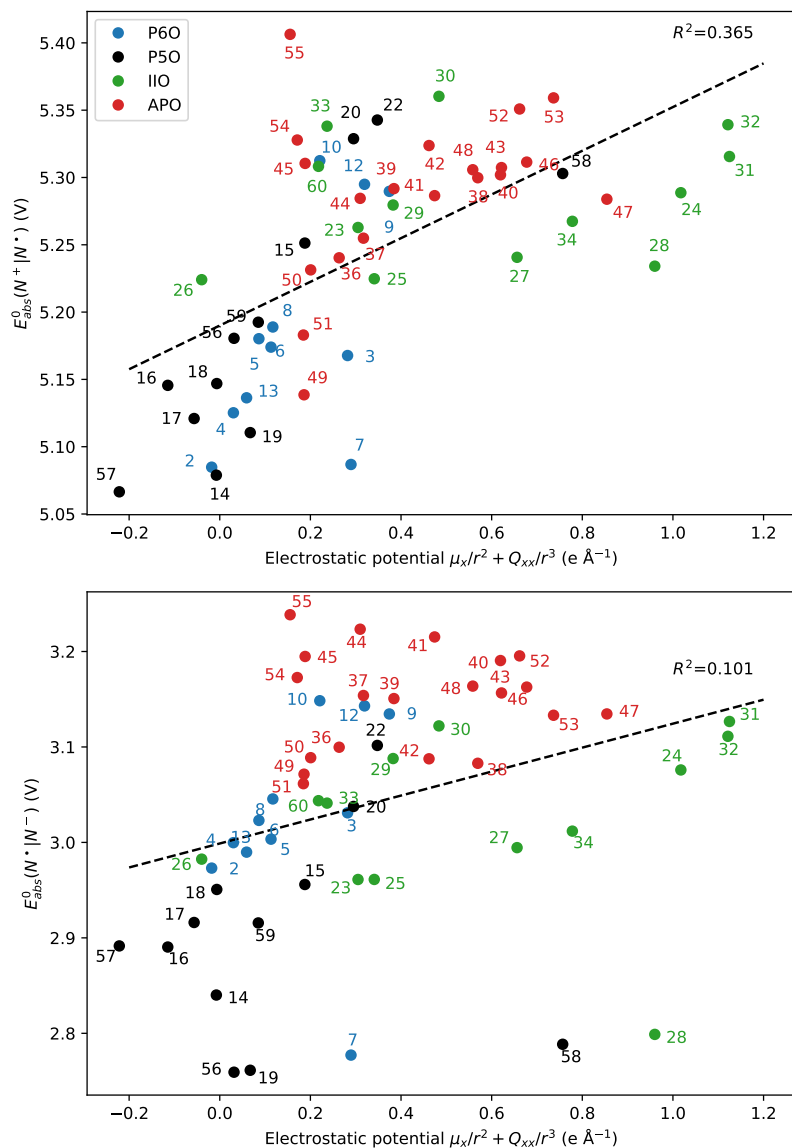


Figure 6: Relationship between absolute oxidation (top) and reduction (bottom) potentials of nitroxides and the electrostatic potential between the redox center ( $>\text{N}-\text{O}^\bullet$ ) and the substituent, as computed at the  $\omega\text{B97X-D/6-311+G(d)}$  level in water (SMD), with  $[\text{X}] = 0 \text{ mol L}^{-1}$ .

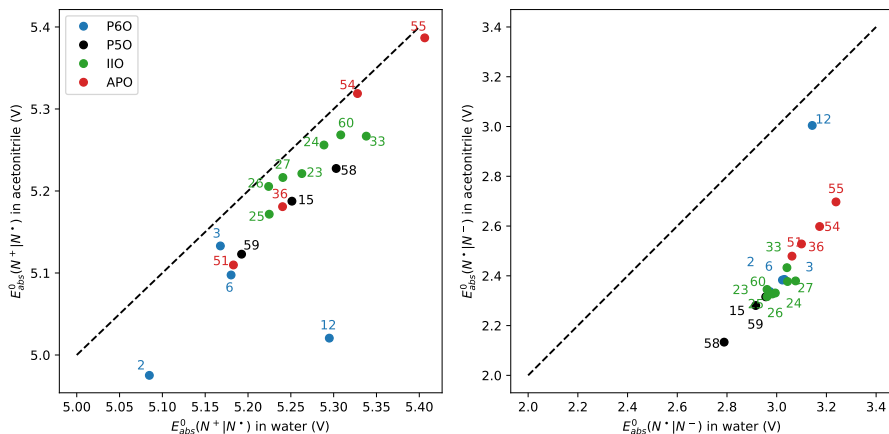


Figure 7: Comparison between absolute oxidation (left) and reduction (right) potentials of nitroxides as computed at the  $\omega$ B97X-D/6-311+G(d) level in water and acetonitrile (SMD), with  $[X] = 0 \text{ mol L}^{-1}$ . The dashed line represents no change.

- [4] J. M. Herbert, Dielectric continuum methods for quantum chemistry, WIREs Computational Molecular Science 11 (2021). doi:10.1002/wcms.1519.
- [5] J. O. Bockris, A. K. N. Reddy, Modern Electrochemistry 1: Ionics, Springer US, Boston, MA, 1998. doi:10.1007/b114546.
- [6] G. M. Kontogeorgis, B. Maribo-Mogensen, K. Thomsen, The Debye-Hückel theory and its importance in modeling electrolyte solutions, Fluid Phase Equilibria 462 (2018) 130–152. doi:10.1016/j.fluid.2018.01.004.
- [7] G. M. Silva, X. Liang, G. M. Kontogeorgis, On the derivations of the Debye-Hückel equations, Molecular Physics 120 (2022) e2064353. doi:10.1080/00268976.2022.2064353.
- [8] M. Cossi, V. Barone, B. Mennucci, J. Tomasi, Ab initio study of ionic solutions by a polarizable continuum dielectric model, Chemical Physics Letters 286 (1998) 253–260. doi:10.1016/S0009-2614(98)00106-7.
- [9] L. Wylie, K. Oyaizu, A. Karton, M. Yoshizawa-Fujita, E. I. Izgorodina,

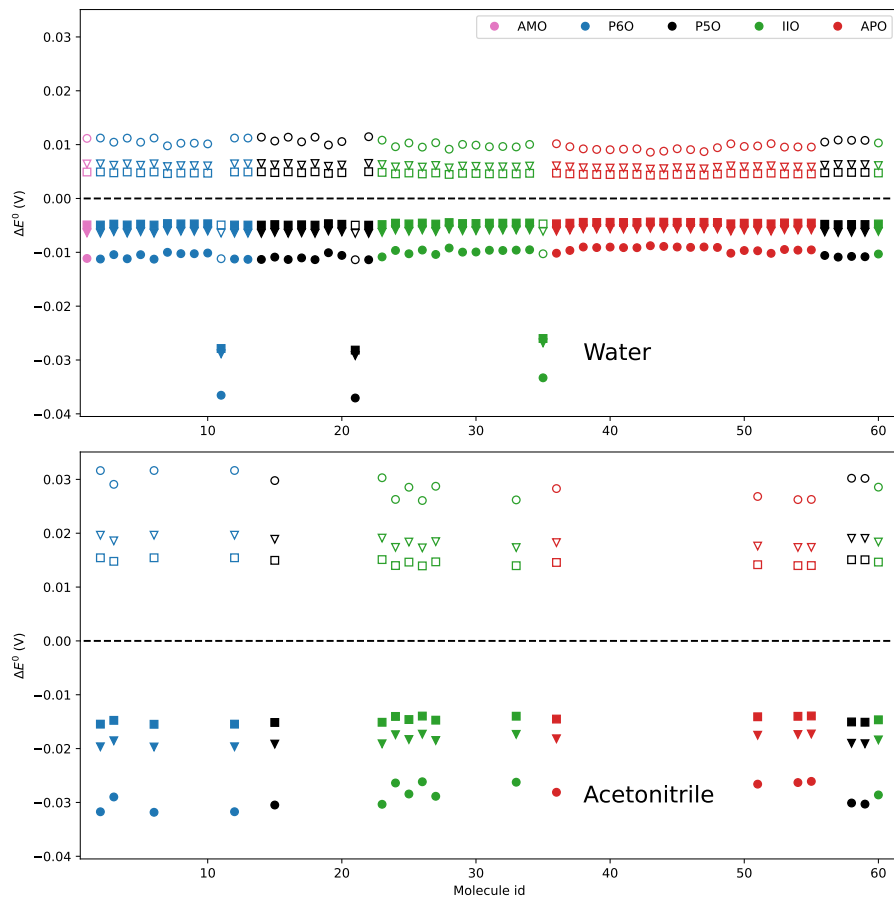


Figure 8: Impact of the Debye-Huckel correction, as  $\Delta E^0 = -\frac{\Delta G_{DH}^*}{F}$  for  $[X] = 1 \text{ mol L}^{-1}$  (round markers),  $[X] = 0.1 \text{ mol L}^{-1}$  (triangular markers) and  $[X] = 0 \text{ mol L}^{-1}$  (square markers), as computed at the  $\omega\text{B97X-D/6-311+G(d)}$  level in water (top) and acetonitrile (bottom) using SMD. Filled (empty) markers represent the correction to the oxidation (reduction) potential.

Toward Improved Performance of All-Organic Nitroxide Radical Batteries with Ionic Liquids: A Theoretical Perspective, ACS Sustainable Chemistry & Engineering 7 (2019) 5367–5375. doi:10.1021/acssuschemeng.8b06393.

- [10] J. L. Hodgson, M. Namazian, S. E. Bottle, M. L. Coote, One-Electron Oxidation and Reduction Potentials of Nitroxide Antioxidants: A Theoretical

- Study, *The Journal of Physical Chemistry A* 111 (2007) 13595–13605. doi:10.1021/jp074250e.
- [11] A. V. Marenich, C. J. Cramer, D. G. Truhlar, Universal Solvation Model Based on Solute Electron Density and on a Continuum Model of the Solvent Defined by the Bulk Dielectric Constant and Atomic Surface Tensions, *The Journal of Physical Chemistry B* 113 (2009) 6378–6396. doi:10.1021/jp810292n.
- [12] M. J. Frisch, G. W. Trucks, H. B. Schlegel, G. E. Scuseria, M. A. Robb, J. R. Cheeseman, G. Scalmani, V. Barone, G. A. Petersson, H. Nakatsuji, X. Li, M. Caricato, A. V. Marenich, J. Bloino, B. G. Janesko, R. Gomperts, B. Mennucci, H. P. Hratchian, J. V. Ortiz, A. F. Izmaylov, J. L. Sonnenberg, D. Williams-Young, F. Ding, F. Lipparini, F. Egidi, J. Goings, B. Peng, A. Petrone, T. Henderson, D. Ranasinghe, V. G. Zakrzewski, J. Gao, N. Rega, G. Zheng, W. Liang, M. Hada, M. Ehara, K. Toyota, R. Fukuda, J. Hasegawa, M. Ishida, T. Nakajima, Y. Honda, O. Kitao, H. Nakai, T. Vreven, K. Throssell, J. A. Montgomery, Jr., J. E. Peralta, F. Ogliaro, M. J. Bearpark, J. J. Heyd, E. N. Brothers, K. N. Kudin, V. N. Staroverov, T. A. Keith, R. Kobayashi, J. Normand, K. Raghavachari, A. P. Rendell, J. C. Burant, S. S. Iyengar, J. Tomasi, M. Cossi, J. M. Millam, M. Klene, C. Adamo, R. Cammi, J. W. Ochterski, R. L. Martin, K. Morokuma, O. Farkas, J. B. Foresman, D. J. Fox, *Gaussian 16 Revision C.02*, 2019. Gaussian Inc. Wallingford CT.
- [13] G. M. Silva, X. Liang, G. M. Kontogeorgis, The true Hückel equation for electrolyte solutions and its relation with the Born term, *Journal of Molecular Liquids* 368 (2022) 120554. doi:10.1016/j.molliq.2022.120554.